

# Moment of Inertia and Dynamical Symmetry

 József Cseh <sup>\*,†</sup> and Gábor Riczu <sup>†</sup> 

Institute for Nuclear Research, P.O. Box 51, 4001 Debrecen, Hungary; riczugabor@atomki.hu

\* Correspondence: cseh@atomki.hu

† These authors contributed equally to this work.

**Abstract:** We investigate how the moment of inertia of the atomic nucleus can be calculated in terms of the invariant operator of its SU(3) symmetry. This question is important for model Hamiltonians containing the moment of inertia explicitly, e.g., those with multichannel dynamical symmetry, which describes many different bands in a unified way.

**Keywords:** moment of inertia; dynamical symmetry; algebraic structure models; rotational spectra

## 1. Introduction

Considering nuclear rotation, two extremes can be identified: rigid rotation and irrotational flow [1–3]. Real nuclei are somewhere between the two limits [4,5]. The more deformed the system, the more rigid-rotor-like it is. Superdeformed bands show rigid-rotor characteristics [6].

The first microscopic explanation of the quadrupole deformation and collective rotation was given by the Elliott model [7–10]. It is a spherical shell model in which the average potential is that of the harmonic oscillator, while the residual interaction is a quadrupole force:

$$H = H_{HO} - \chi q^a q^a. \quad (1)$$

Here,  $q^a$  is the algebraic mass quadrupole momentum (which is discussed in more detail later on). It can be expressed in terms of the invariant operators of the SU(3) and SO(3) algebras

$$q^a q^a = 6C_{SU3}^{(2)} - 3C_{SO3}^{(2)}. \quad (2)$$

Here,  $C$  stand for the Casimir operators of the Lie groups, indicated as subscripts, while the order of the invariant is given as a superscript. The harmonic oscillator (HO) Hamiltonian is the invariant of the U(3) algebra; therefore, the Hamiltonian (1) is

$$H = \hbar\omega C_{U3}^{(1)} - 6\chi C_{SU3}^{(2)} + 3\chi C_{SO3}^{(2)}. \quad (3)$$

Since it is expressed in terms of the Casimir invariants of a single algebra chain of

$$U(3) \supset SU(3) \supset SO(3), \quad (4)$$

it is said to have a U(3) dynamical symmetry. The quantum numbers characterizing these symmetries are as follows—U(3):  $[n_1, n_2, n_3]$ , SU(3):  $(\lambda, \mu)$ , SO(3):  $L$ .

The invariant operator of the rotational algebra is  $C_{SO3}^{(2)} = L^2$ , and the moment of inertia  $\theta$  is determined by its coefficient in Equation (3):  $\frac{1}{2\theta} = 3\chi$ . As is obvious from Equation (3), this model gives a uniform moment of inertia for all the rotational bands of a nucleus [11].

The Elliott model is a single-shell model in its original form, and, following its introduction, it was applied mainly to problems containing only a few collective bands. Later on, several extensions have been invented [12–15]. (For a brief recent review, see, e.g., [16]).



**Citation:** Cseh, J.; Riczu, G. Moment of Inertia and Dynamical Symmetry. *Symmetry* **2023**, *15*, 2116. <https://doi.org/10.3390/sym15122116>

Academic Editor: Anna Cimmino

Received: 26 October 2023

Revised: 12 November 2023

Accepted: 22 November 2023

Published: 27 November 2023



**Copyright:** © 2023 by the authors. Licensee MDPI, Basel, Switzerland. This article is an open access article distributed under the terms and conditions of the Creative Commons Attribution (CC BY) license (<https://creativecommons.org/licenses/by/4.0/>).

Here, we concentrate on the multiconfigurational dynamical symmetry (MUSY) [17,18], which is the common intersection of the shell, collective and cluster models for multi-major-shell problems. Therefore, it is able to give a unified description of spectra of wide energy and deformation regions for different configurations, e.g., shell, core-plus-alpha or exotic clusters. Obviously, under these circumstances, a uniform moment of inertia would be an extremely poor approximation.

Surprisingly enough, however, a very simple Hamiltonian can perform well in describing such spectra. This is a gentle extension of Equation (3), as follows:

$$H = \hbar\omega n + aC_{SU3}^{(2)} + bC_{SU3}^{(3)} + d\frac{1}{2\theta}L^2. \quad (5)$$

The new aspects, in comparison with the original Hamiltonian of the Elliott model, are (i) the inclusion of a third order term  $C_{SU3}^{(3)}$ , which makes a distinction between prolate and oblate deformation and (ii) the fact that, in the rotational term, the moment of inertia is no longer uniform. Rather, it is calculated for an ellipsoidal shape defined by the U(3) quantum numbers. The expectation values of the  $C_{SU3}^{(2)}$  and  $C_{SU3}^{(3)}$  Casimir invariants in the SU(3) basis with  $(\lambda, \mu)$  quantum numbers are  $\lambda^2 + \mu^2 + \lambda\mu + 3(\lambda + \mu)$  and  $(\lambda - \mu)(\lambda + 2\mu + 3)(2\lambda + \mu + 3)$ , respectively.

This Hamiltonian is invariant with respect to the transformations from one configuration to the other [19], and its eigenvalue problem has an analytical solution in the U(3) basis. In this sense, one can say that it is a Hamiltonian with a dynamical symmetry of group-chain (4). Nevertheless, it does not correspond to the strict definition of the dynamical symmetry, which requires that the Hamiltonian is expressed in terms of the invariant operators of a group-chain [20] (due to the method of performing the calculation of the moment of inertia).

In this work, we investigate what kind of description of the experimental spectra can be obtained with Hamiltonians in which the moment of inertia is given in terms of the second-order Casimir of SU(3) [21,22], i.e., the Hamiltonians have dynamical symmetries in the strict sense.

Please note that the Elliott model and many other shell models, as well as our approach presented here, describe the nuclear rotation in the laboratory frame of reference. There is, however, a different possible route for treating this problem, namely, describing the nucleon motion in a rotating frame. In that case, centrifugal and Coriolis forces emerge, and these give rise to a different approach towards moment of inertia. Here, we focus on the Elliott-type treatment. For a recent study with cranking models, we refer the reader to work [23] and the references therein. Another interesting relationship between the nuclear rotation and the magnetic effects is discussed in [24].

In what follows, we first recall some basic relation of the quadrupole moment and moment of inertia in Section 2. Then, in Section 3, we compare the moment of inertia of the rigid ellipsoid with those expressed in terms of the Casimir invariant. In Section 4, we describe some experimental data with the strictly dynamically symmetric Hamiltonians. Finally, a brief summary is given and some conclusions are drawn in Section 5.

## 2. Rigid Body: Quadrupole Moment and Moment of Inertia

### 2.1. Quadrupole Moment

Both the moment of inertia and the quadrupole moment are second-rank tensors. The Cartesian components of the quadrupole moment of  $N$  points (of mass  $m_n$ ), or a distribution of matter of density  $\rho$ , are [25]

$$Q_{ij} = \sum_n m_n x_{ni} x_{nj}, \text{ or } \int x_i x_j \rho(\mathbf{r}) dv, \quad i, j = 1, 2, 3. \quad (6)$$

This is a symmetric tensor with six independent components. It can be split up into a zeroth- and a second-rank spherical tensor with one and five components, respectively.

The scalar ( $L = 0$ ) monopole moment is

$$M = \sum_i Q_{ii}. \quad (7)$$

The five  $q_m$  components of the  $L = 2$  irreducible tensor transform according to the irreducible representation  $\mathcal{D}^2$  of the rotation group [26]

$$q'_{m'} = \sum_m q_m \mathcal{D}_{mm'}^2(\alpha\beta\gamma), \quad (8)$$

where  $(\alpha\beta\gamma)$  are the Euler angles of the rotation. Their relations to the Cartesian components are

$$\begin{aligned} q_0 &= \sqrt{\frac{5}{16\pi}}(2Q_{33} - Q_{11} - Q_{22}) \\ q_{\pm 1} &= \mp \sqrt{\frac{15}{8\pi}}(Q_{31} \pm iQ_{32}) \\ q_{\pm 2} &= \sqrt{\frac{15}{32\pi}}(Q_{11} - Q_{22} \pm 2iQ_{12}). \end{aligned} \quad (9)$$

In terms of the spherical harmonics, they are [25]

$$q_m = \sum_n m_n r_n^2 Y_{2m}(\theta_n, \phi_n), \text{ or } \int r^2 Y_{2m}(\theta, \phi) \rho(\mathbf{r}) dv. \quad (10)$$

## 2.2. Moment of Inertia

The Cartesian coordinates of the moment of inertia tensor of a rigid body are [27,28]

$$I_{ij} = \sum_n m_n (r_n^2 \delta_{ij} - x_i x_j), \text{ or } \int (r^2 \delta_{ij} - x_i x_j) \rho(\mathbf{r}) dv. \quad (11)$$

The scalar moment of inertia  $I$  for any axis  $\mathbf{v}$  is obtained as a double scalar product:

$$I = \mathbf{v} \hat{I} \mathbf{v} = \sum_{j=1}^3 \sum_{k=1}^3 v_j I_{jk} v_k. \quad (12)$$

The moment of inertia of a cylindrically symmetric ellipsoid of major axes  $a$  and  $b = c$  (which can rotate around an axis perpendicular to its symmetry axis  $a$ ) is

$$(\theta =) I_c = \frac{1}{5} m (a^2 + b^2). \quad (13)$$

Its unit is  $\frac{\hbar^2}{MeV}$ . If the  $U(3)$  symmetry is  $[n_1, n_2, n_3]$ , then  $a, b, c$  are obtained from the self-consistency argument [29]:

$$\frac{a}{c} = \frac{n_1 + \frac{A}{2}}{n_3 + \frac{A}{2}}, \quad \frac{b}{c} = \frac{n_2 + \frac{A}{2}}{n_3 + \frac{A}{2}} \quad (14)$$

and the volume-conservation requirements:

$$c = R_0^3 \sqrt[3]{A \frac{(n_3 + \frac{A}{2})^2}{(n_1 + \frac{A}{2})(n_2 + \frac{A}{2})}} \quad (15)$$

Here,  $A$  is the number of nucleons and  $R_0$  is the radius parameter (typically 1.2 fm). The approximation of the cylindrical symmetry is needed in order to have an analytical solution for the energy eigenvalue.

The moments of inertia of an ellipsoid without cylindrical symmetry are

$$\begin{aligned}
 I_a &= \frac{1}{5}m(b^2 + c^2) \\
 I_b &= \frac{1}{5}m(a^2 + c^2) \\
 I_c &= \frac{1}{5}m(a^2 + b^2)
 \end{aligned} \tag{16}$$

### 2.3. Relation of the Two Moments

The relation of the tensors of the quadrupole moment and the moment of inertia is

$$Q_{ij} = \frac{1}{2}Tr(\hat{I})\delta_{ij} - I_{ij}. \tag{17}$$

In the reference frame of principal axes, both tensors are diagonal. Then, the quadrupole components expressed with the  $I_{ii} = I_i$  moments of inertia are

$$\begin{aligned}
 Q_{11} &= \frac{1}{2}(-I_1 + I_2 + I_3), \\
 Q_{22} &= \frac{1}{2}(I_1 - I_2 + I_3), \\
 Q_{33} &= \frac{1}{2}(I_1 + I_2 - I_3),
 \end{aligned} \tag{18}$$

or, with  $Q_{ii} = \lambda_i$ , are

$$\begin{aligned}
 I_{11} &= (\lambda_2 + \lambda_3), \\
 I_{22} &= (\lambda_1 + \lambda_3), \\
 I_{33} &= (\lambda_1 + \lambda_2).
 \end{aligned} \tag{19}$$

### 2.4. Shell Connection

The  $\lambda_i$  quadrupole values can be related to the shell-model picture too [6]. First, it should be noted that, in the shell model, two different quadrupole operators can be constructed. The physical (or collective) one has non-vanishing matrix elements between basis states of the same major shell, as well as between those of the shells with two more or two fewer quanta. (Sometimes, this is denoted by  $Q^c$ . In our notation,  $Q^c \equiv Q$ .) The spherical coordinates of the physical quadrupole moment of  $A$  nucleons in a harmonic oscillator potential with parameter  $b = \sqrt{\hbar/m\omega}$  are

$$q_m = \sqrt{\frac{16\pi}{5}} \sum_{n=1}^A \frac{r_n^2}{b^2} Y_{2m}(\theta_n, \phi_n). \tag{20}$$

There is an algebraic approximation to this,  $q^a$ , introduced in the Elliott model, which has the same matrix elements within the major shell, but all its matrix elements vanish between states of different shells. It contains the space and momentum coordinates in a symmetric way:

$$q_m^a = \sqrt{\frac{4\pi}{5}} \sum_{n=1}^A \left( \frac{r_n^2}{b^2} Y_{2m}(\theta_n, \phi_n) + b^2 p_n^2 Y_{2m}(\theta_n^p, \phi_n^p) \right). \tag{21}$$

(the different spectra obtained with the collective and algebraic quadrupole moments were studied numerically and analytically in refs. [30,31], respectively.)  $q_m^a$  generate the SU(3) group together with the angular momentum operators, i.e., they give the Lie algebra of SU(3). On the other hand, the commutation relations of the components of  $q^c$  are different. In a unified notation, in which  $q^\chi$  stands for either  $q^c \equiv q$  or for  $q^a$ ,

$$[L_\mu, L_\nu] = -\sqrt{2}\langle 1\mu, 1\nu | 1\mu + \nu \rangle L_{\mu+\nu}, \tag{22}$$

$$[L_\mu, q_\nu^\chi] = \sqrt{6}\langle 1\mu, 2\nu | 2\mu + \nu \rangle q_{\mu+\nu}^\chi, \tag{23}$$

$$[q_\mu^\chi, q_\nu^\chi] = c \langle 2\mu, 2\nu | 1\mu + \nu \rangle L_{\mu+\nu}, \tag{24}$$

where  $c = 0$  for the physical quadrupole operators ( $q^c$ ), while, for the algebraic ( $q^a$ ) ones,  $c = 3\sqrt{10}$ . The  $\langle | \rangle$  symbol shows the Clebsch–Gordan coefficients. For  $c = 0$ , the operators generate the  $T_5 \wedge SO(3)$  group of the rigid rotor (of semi-direct product structure), where  $T_5$  stands for the (Abelian) subgroup of  $q_i^c$ s. If one renormalizes  $q^a$  as  $q^a / \sqrt{C_{SU3}^2}$ , then the first and second lines of commutators remain unchanged, while  $L_{\mu+\nu}$  in the third line is substituted by  $L_{\mu+\nu} / C_{SU3}^2$ , which progresses to zero for low  $L$ -s and large  $C_{SU3}^2$ . This procedure is called the contraction of  $SU(3)$  to  $T_5 \wedge SO(3)$ .

The quadrupole moments of the body-fixed principle axes are determined by the  $SU(3)$  quantum numbers as follows [6]:

$$\lambda_1 = -(\lambda - \mu) / 3, \tag{25}$$

$$\lambda_2 = -(\lambda + 2\mu + 3) / 3, \tag{26}$$

$$\lambda_3 = (2\lambda + \mu + 3) / 3. \tag{27}$$

### 2.5. Energy

The energy-operator of a rigid rotor in terms of body-fixed components of the angular momenta ( $L'_i$ ) is

$$H = \frac{L_1'^2}{2I_1} + \frac{L_2'^2}{2I_2} + \frac{L_3'^2}{2I_3}. \tag{28}$$

This can be rewritten [6] in a frame-independent form with the three scalars,

$$L^2 = \sum_i L_i^2 = \sum_i L_i'^2, \tag{29}$$

$$X_3 = \sum_{ij} L_i Q_{ij} L_j = \sum_i \lambda_i L_i'^2, \tag{30}$$

$$X_4 = \sum_{ijk} L_i Q_{ij} Q_{jk} L_k = \sum_i \lambda_i^2 L_i'^2, \tag{31}$$

as follows:

$$H = aL^2 + bX_3 + cX_4. \tag{32}$$

### 3. Classical Ellipsoid versus $C^{(2)}$

Here, we compare the moment of inertia of ellipsoids calculated classically with those obtained using different functionals of the invariant operators. In particular, we apply the MUSY Hamiltonian in Equation (5) and calculate the moment of inertia first for ellipsoids, then from the eigenvalues of the invariant operators. So far, we have used the first method in MUSY applications. As mentioned previously, the nucleus is approximated by a cylindrically symmetric one in the case of a triaxial ellipsoid. If the semi-axis lengths of the triaxial nucleus are  $a, b, c$ , then one can make the following approximation for a cylindrically symmetric shape with semi-axis lengths  $A, B, C$ : if  $a/b \geq b/c$ , then  $A = a$  and  $B = C = \sqrt{bc}$ ; otherwise,  $A = B = \sqrt{ab}$  and  $C = c$ .

We consider here the shapes of those nuclei, which were treated in detail by MUSY, i.e., their rich experimental spectra were reproduced in terms of MUSY. These are the  $^{20}\text{Ne}$ , [18,32]  $^{28}\text{Si}$ , [18,33,34]  $^{36}\text{Ar}$ , [18,34,35] and  $^{44}\text{Ti}$  nuclei [17,18,34].

As for the functional forms of invariant operators, we take the simplest ones:

- (i) Second-order Casimir of  $SU(3)$  ( $a_1 C_{SU(3)}^{(2)}$ );
- (ii) ( $a_0 + a_1 C_{SU(3)}^{(2)}$ );
- (iii) ( $a_1 C_{SU(3)}^{(2)} + a_2 n$ ), where  $n$  is the linear Casimir of  $U(3)$ ;

(iv)  $(a_0 + a_1 C_{SU(3)}^{(2)} + a_2 n)$ .

Figure 1 shows the comparison between the different values of moment of inertia for those shapes of nuclei which have experimental counterparts. The  $a_i$  parameters were determined from a fit to the ellipsoidal values. These figures suggest that the simple two-parameter formula  $a_0 + a_1 C_{SU(3)}^{(2)}$  approximates the ellipsoidal value very well.

The shapes observed experimentally are rather different from each other in all these nuclei; therefore, the systematic change of the moment of inertia as a function of the deformation is not shown by these figures. In order to see this, we made another comparison between the ellipsoidal and invariant values. In particular, we changed the quantum numbers of the SU(3) symmetry step-by-step, in order to study the behavior in the different functions. We kept the  $n$  number constant and changed the distribution among its Cartesian components in such a way that the deformation shows a smooth change (we have chosen the sets of U(3) quantum numbers for  $2\hbar\omega$  excitation in each nucleus).

We looked at the systematic change of the prolate, triaxial and oblate shapes between large and small deformations. These SU(3) irreducible representations and the corresponding quadrupole shapes are not necessarily physical, of course. The purpose of this comparison was simply to study the similarity or difference among the different functional forms. Figure 2 shows the result. This comparison also prefers the simple  $a_0 + a_1 C_{SU(3)}^{(2)}$  functional form for the calculation of the moment of inertia in terms of invariant operators. (Please note that the two other functions in Figure 1 do not represent independent choice, in this case, due to the constant  $n$  values.)

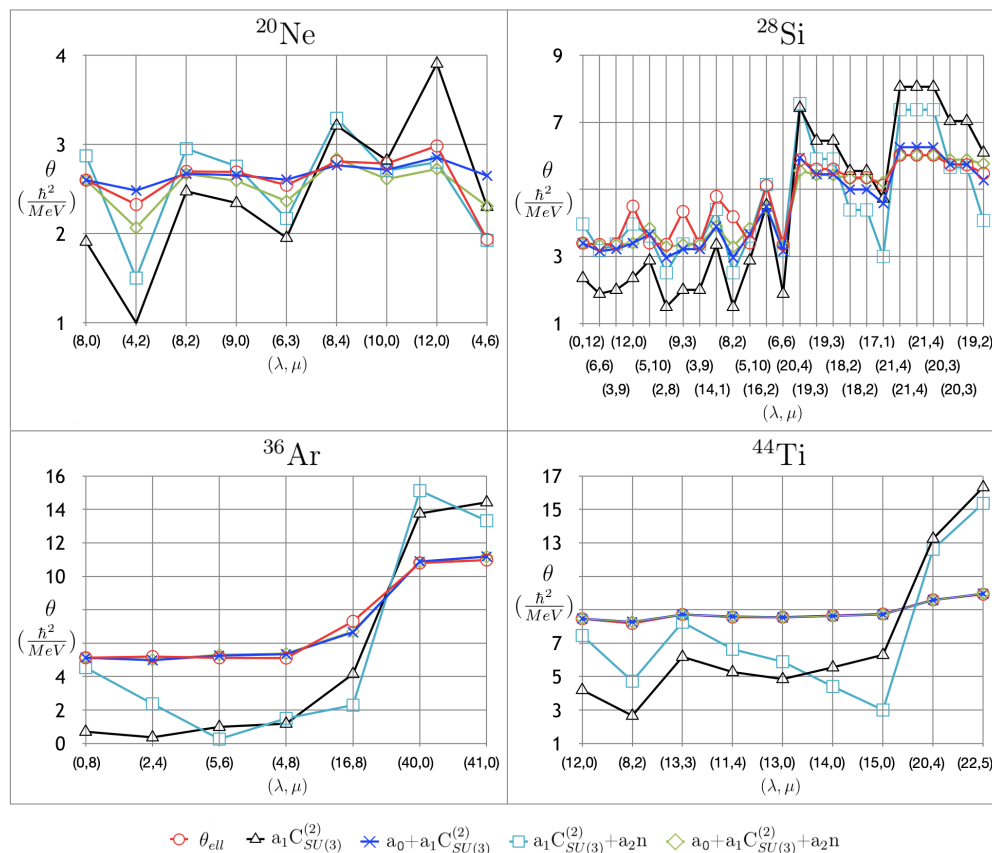


**Figure 1.** Nuclear moment of inertia calculated using different methods. The SU(3) quantum numbers (quadrupole shapes) that are shown seem to have experimental counterparts (see text for more details). Red circles indicate the values calculated classically (for an ellipsoid with cylindrical symmetry), while black triangles, dark blue stars, light blue squares and green diamonds are those calculated with Casimir operators.

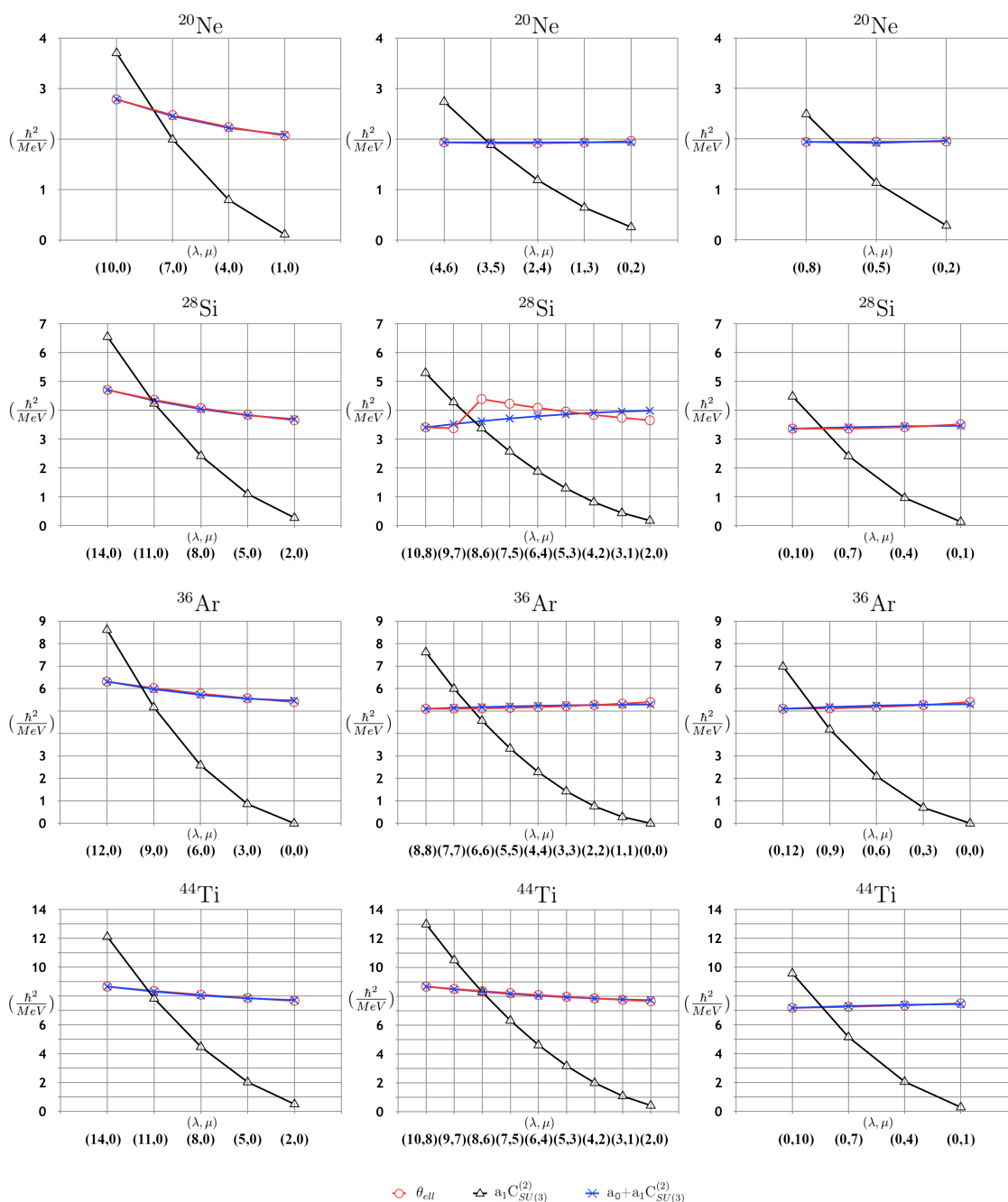


**Figure 2.** Moment of inertia, calculated by different methods, for prolate (left), triaxial (middle) and oblate (right) shapes of gradually decreasing deformation.

### 4. Energy Spectra

We calculated energy spectra for four nuclei with different moments of inertia and B(E2) transitions (Tables 1 and 2). On the one side, we applied the ellipsoid values, as was performed previously; on the other side, we calculated the moment of inertia using two functionals with the Casimir invariant. The parameters of the Hamiltonian were fitted to the experimental data, where the goodness of fit is as follows:

$$F = \sum_{i=1}^m w_i \frac{(E_i^{th} - E_i^{exp})^2}{(E_i^{exp})^2} \tag{33}$$

Here,  $m$  is the number of states and  $w_i$ ,  $E_i^{th}$  and  $E_i^{exp}$  are the weights, theoretical energies and experimental energies of the states.

In some cases ( $^{28}\text{Si}$ ,  $^{44}\text{Ti}$ ), the two methods resulted in similar fits between the experimental data and the model spectra. In other cases, however, the purely algebraic calculations (with invariant operators) gave a considerably better fit (ca. a factor of 2 for  $^{20}\text{Ne}$  and a factor of 4 for  $^{36}\text{Ar}$ ).

Figures 3–6 show the results of the calculation with the moment of inertia  $\theta = a_0 + a_1 C_{SU3}^{(2)}$ . In the fitting procedure, the weights of the bands are as follows:  $^{20}\text{Ne}$ —all bands have a unit weight;  $^{28}\text{Si}$ —all low-energy bands have a unit weight and the resonances have a weight of 0;  $^{36}\text{Ar}$ —the well-known GB and SD bands have a unit weight, while the other bands have a weight of 0.01;  $^{44}\text{Ti}$ —the well-known states have a unit weight (first three states of GB and  $0_2^+$  bands, first states of  $3^-$  and  $4^-$  bands, first  $\alpha$  band,  $5^-$  state of last  $\alpha$  band), while the states with uncertain spin parity and the resonances have a weight of 0.5. When there is more than one candidate for the state in an alpha-cluster band, the unit weight was divided by their number.

The in-band B(E2) value is given as

$$B(E2, L_i \rightarrow L_f) = \frac{2L_f + 1}{2L_i + 1} \alpha^2 |\langle (\lambda\mu)KL_i, (11)2 || (\lambda\mu)KL_f \rangle|^2 C_{SU(3)}^2 \tag{34}$$

where  $\langle (\lambda\mu)KL_i, (11)2 || (\lambda\mu)KL_f \rangle$  is a  $SU(3) \supset SO(3)$  Wigner coefficient [36] and  $\alpha^2$  (measured in W.u.) is a parameter fitted to the lowest transition of the ground band for each nucleus (Tables 1 and 2).

This formula explains why the transition strength can be very large for the extremely deformed (superdeformed, hyperdeformed, etc.) bands (c.f.  $C_{su(3)}^2$ ), as well as for the fine details within a rotational band (Wigner coefficients). Within the dynamical symmetry approach, applied here with one-body transition operators [32,33], the interband transitions are forbidden (they could be achieved either with symmetry-breaking or with transition operators of higher order).

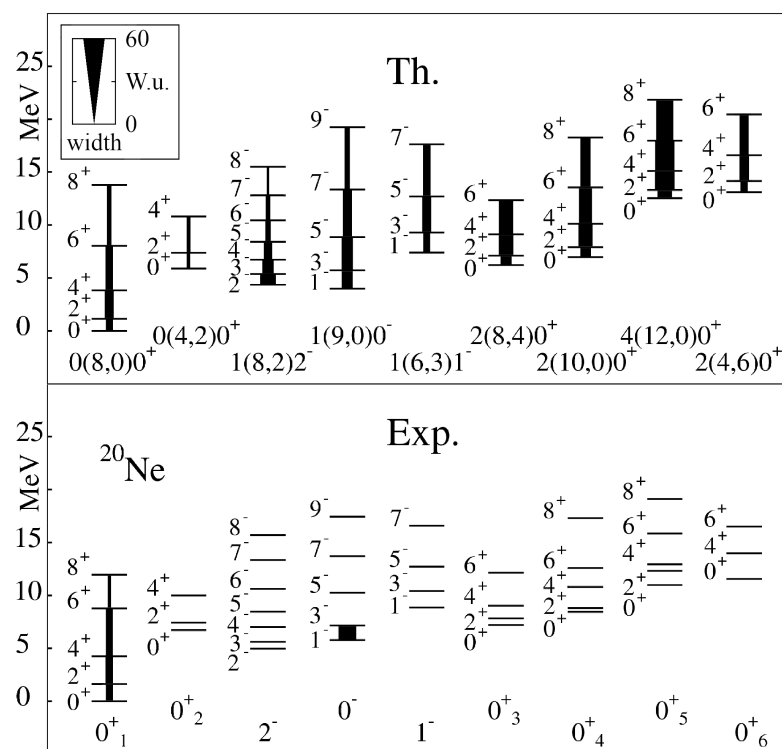


**Figure 3.** The spectrum of the MUSY (upper part) in comparison with the experimental data of the  $^{20}\text{Ne}$  nucleus (lower part). The experimental bands are labeled by the  $K^\pi$ , and the model states by the  $n(\lambda\mu)K^\pi$  quantum numbers. The width of the arrow between the states is proportional to the strength of the E2 transition.

**Table 1.** The experimentally known B(E2) transitions in the investigated nuclei and their theoretical counterparts.

Nucleus	Band	$L_1^\pi \rightarrow L_2^\pi$	$B(E2)_{exp.}(W.u.)$	$B(E2)_{th.}(W.u.)$
$^{20}\text{Ne}$	$0_1^+$	$2^+ \rightarrow 0^+$	20.3	20.3
		$4^+ \rightarrow 2^+$	22	25.7
		$6^+ \rightarrow 4^+$	20	21.8
		$8^+ \rightarrow 6^+$	9	12.9
	$0^-$	$3^- \rightarrow 1^-$	50	30.8
$^{28}\text{Si}$	GB	$2^+ \rightarrow 0^+$	13.2	13.2
		$4^+ \rightarrow 2^+$	16.4	17.8
		$6^+ \rightarrow 4^+$	10.6	17.5
	$\beta 0^+$	$2^+ \rightarrow 0^+$	5.0	8.2
	$(12,0)0^+$	$4^+ \rightarrow 2^+$	30.4	17.8
		$6^+ \rightarrow 4^+$	37	17.5
O+P3 $^-$	$4^- \rightarrow 3^-$	0.91	24.7	
$^{36}\text{Ar}$	GB	$2^+ \rightarrow 0^+$	8.2	8.2
		$4^+ \rightarrow 2^+$	12	10.4
	$2^+$	$3^+ \rightarrow 2^+$	0.29	6.8
	$3^-$	$4^- \rightarrow 3^-$	0.35	15.6
	SD	$4^+ \rightarrow 2^+$	53	60.9
		$6^+ \rightarrow 4^+$	64	65.6
		$8^+ \rightarrow 6^+$	62	66.5
		$10^+ \rightarrow 8^+$	45	65.6
		$12^+ \rightarrow 10^+$	39	63.5
		$14^+ \rightarrow 12^+$	33	60.3
$16^+ \rightarrow 14^+$	18	55.9		
$^{44}\text{Ti}$	GB	$2^+ \rightarrow 0^+$	13	13.0
		$4^+ \rightarrow 2^+$	10	17.5
	$0_2^+$	$2^+ \rightarrow 0^+$	23	7.8
		$4^+ \rightarrow 2^+$	21	10.5

**Table 2.** Parameters of the Hamiltonian and the B(E2) transitions and the quality of the fit for different moments of inertia. For each nucleus, the first row shows the results of the 4-parameter fitting, where the moment of inertia is calculated for a rigid ellipsoid. The second and third rows show the results of simultaneous fitting of parameters of  $\theta$  and  $\hbar\omega$ , a, b (in the latter cases, d = 1 was fixed).

Nucleus	$\alpha^2$	$\theta$	$\hbar\omega$	a	b	d	F
$^{20}\text{Ne}$	1.153	$\theta_{ell}$	6.66030	-0.14261	0.00000	0.94185	1.13874
		$0.028457C_{SU(3)}^2$	6.152410	-0.090513	-0.000971	1	0.70997
		$1.398849 + 0.013758C_{SU(3)}^2$	6.403456	-0.108297	-0.000973	1	0.66174
$^{28}\text{Si}$	0.366	$\theta_{ell}$	5.51017	-0.07859	0.00062	1.44233	0.82616
		$0.013176C_{SU(3)}^2$	6.168610	-0.074770	0.000526	1	1.00443
		$1.461578 + 0.005352C_{SU(3)}^2$	6.447891	-0.081092	0.000530	1	0.98845

Table 2. Cont.

Nucleus	$\alpha^2$	$\theta$	$\hbar\omega$	a	b	d	F
$^{36}\text{Ar}$	0.466	$\theta_{ell}$	6.52745	-0.06131	0.00032	1.29616	0.92377
		$0.020933C_{SU(3)}^2$	3.497172	-0.028190	0.000250	1	0.38433
		$1.401125 + 0.008935C_{SU(3)}^2$	3.036900	-0.028339	0.000288	1	0.21183
$^{44}\text{Ti}$	0.361	$\theta_{ell}$	5.90654	-0.07512	0.00104	1.23395	1.37327
		$0.030113C_{SU(3)}^2$	6.133733	-0.084859	0.001472	1	1.45992
		$5.672361 + 0.005232C_{SU(3)}^2$	5.865533	-0.073725	0.001044	1	1.32555

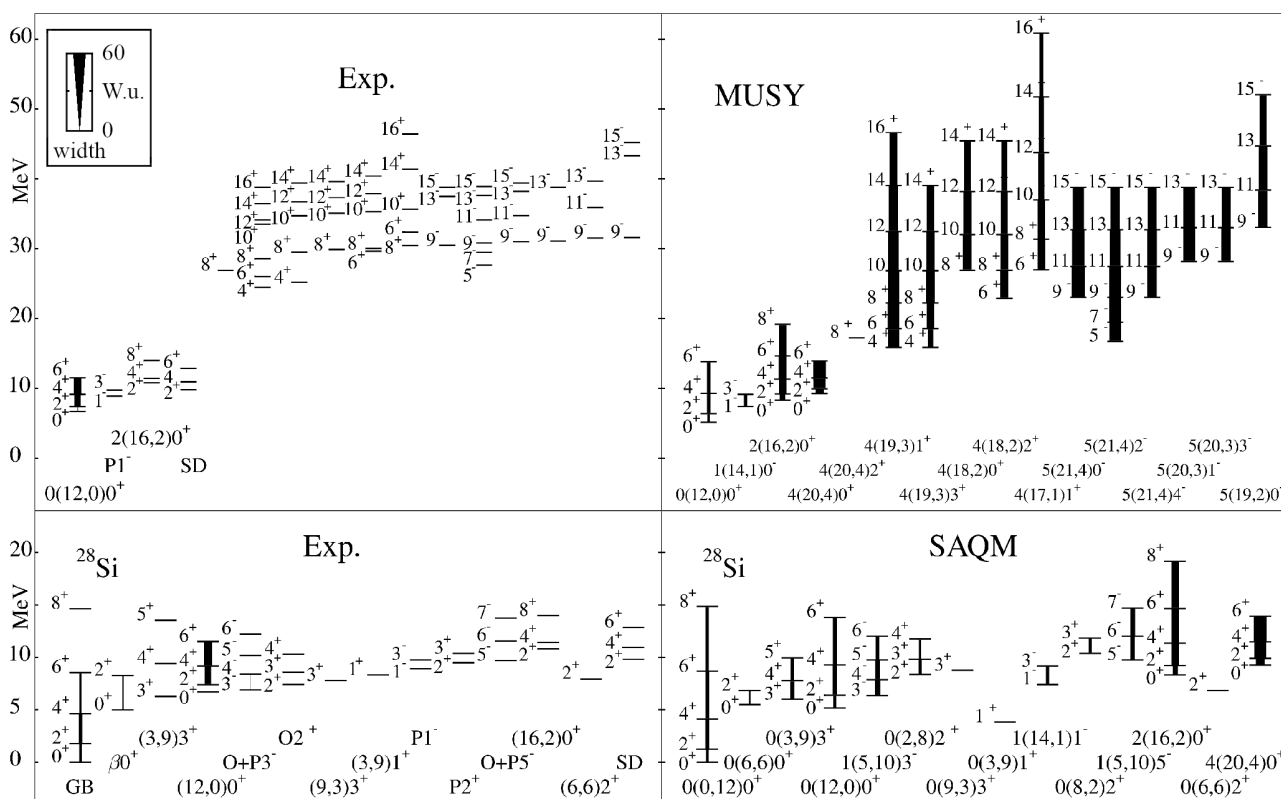
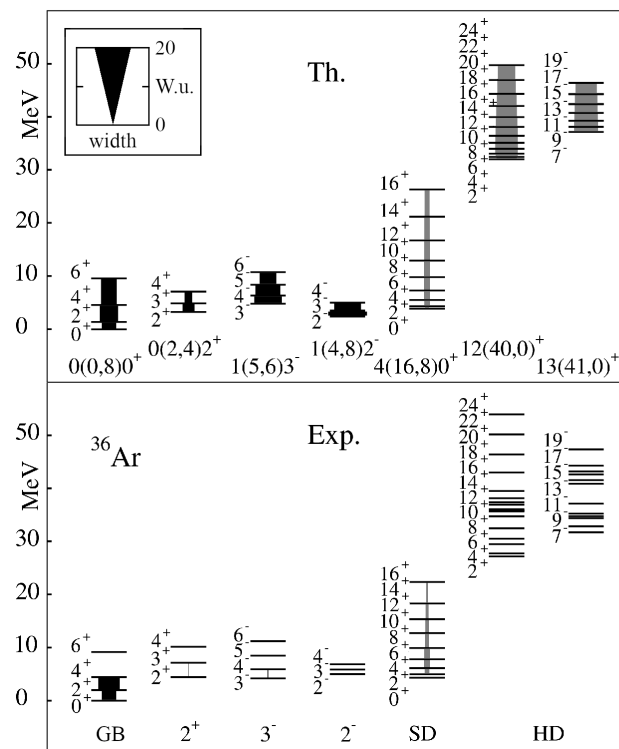
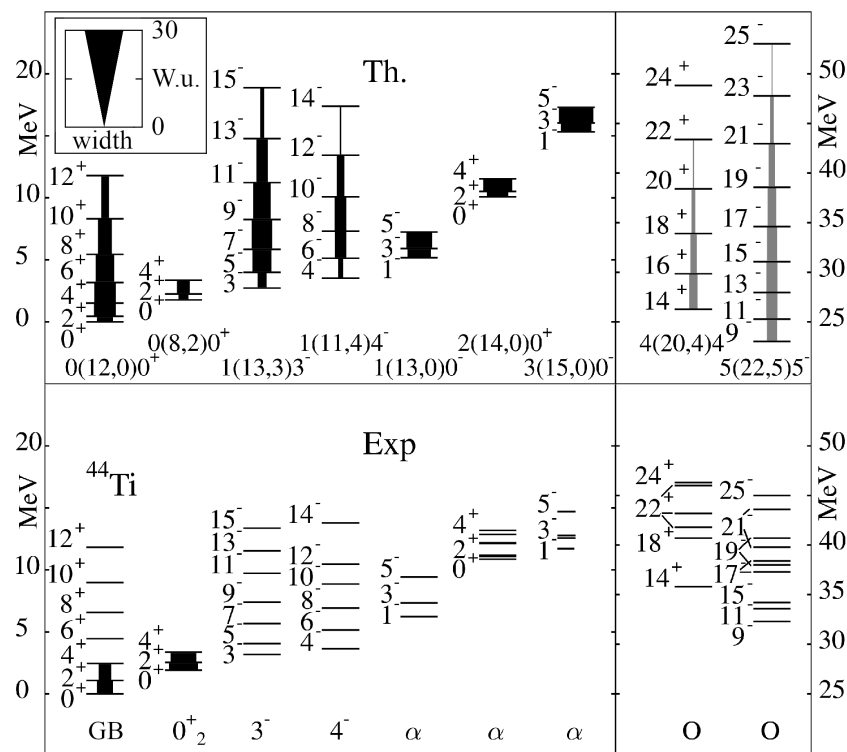


Figure 4. The spectrum of the MUSY in comparison with the experimental data of the  $^{28}\text{Si}$  nucleus. The experimental bands are labeled by the available quantum numbers (GB stands for ground band,  $\beta$  for  $\beta$ -band, P indicates prolate, while O means oblate and SD is superdeformed). The other notations are the same as Figure 3. The parameters have been fitted to the low-energy part (lower panel), and the cluster spectrum (upper panel) is obtained as a pure prediction, due to the unified multiplet structure and identical physical operators.

In this paper, we have considered four nuclei with  $N = Z$ . It should be mentioned, however, that the method is not restricted to such nuclei. Nuclei with different proton and neutron numbers, as well as even and odd mass numbers, are available for MUSY studies. Our present choice was motivated by the methodological nature of this study: we wished to calculate the algebraic moment of inertia for nuclei which have been described beforehand by applying an ellipsoidal approximation.



**Figure 5.** The spectrum of the MUSY in comparison with the experimental data of the  $^{36}\text{Ar}$  nucleus. The notations are the same as Figure 3. The real strength of the gray arrows (of the SD and HD bands) are 20 times the value of the illustrated ones.



**Figure 6.** The spectrum of the MUSY in comparison with the experimental data for the  $^{44}\text{Ti}$  nucleus. In the experimental spectrum,  $\alpha$  indicates the alpha-cluster states, while O means the  $^{28}\text{Si}+^{16}\text{O}$  resonances. The other notations are the same as Figure 3. The real strength of the gray arrows ( $^{16}\text{O}$  bands) is five times the strength of the illustrated ones.

## 5. Summary and Conclusions

In this work, we have investigated the possibility of calculating the moment of inertia of the nucleus in terms of the invariant operator of its SU(3) symmetry.

The inspiration came from the recent applications of multiconfigurational dynamical symmetry. This is the bridge between the shell, collective and cluster models for the multi-major-shell problem. Therefore, it can describe different parts of the nuclear spectrum in a unified way, though they are observed in different reactions and extend along the excitation energy and quadrupole deformation axes. Nevertheless, a simple symmetric Hamiltonian seems to be able to reproduce their gross features. It is only slightly more general than that using the Hamiltonian from the Elliott model. The main difference is that it includes the moment of inertia explicitly; therefore, the rotational bands show different characteristics. The moment of inertia was calculated classically for an ellipsoid, determined by the U(3) symmetry of the band. Here, we addressed the question as to what kind of description of the experimental spectra could be obtained by expressing the moment of inertia in a purely algebraic (quantum mechanical) way.

After reviewing some basic relations between the quadrupole and moment of inertia tensors, we tested the performance of a few simple functional forms of the second-order Casimir of SU(3). We found that the  $\theta = a_0 + a_1 C_{SU3}^{(2)}$  expression gives a very good description of the ellipsoid values, both for the specific bands of the nuclei investigated so far with MUSY and for the systematic behavior of the moment of inertia (as a function of the deformation). As for the description of the experimental data, in some cases, the two methods gave similar fits, while, in other cases, the invariant operators resulted in considerably better agreement.

Based on the present study, an explicit expression of the moment of inertia in terms of the invariant operator of SU(3) seems to be a good candidate for a dynamically symmetric Hamiltonian.

**Author Contributions:** J.C.: Conceptualization, methodology, writing; G.R.: Investigation, software, numerical calculations, visualization. All authors have read and agreed to the published version of the manuscript.

**Funding:** This work was supported by the National Research, Development and Innovation Fund of Hungary, financed under the K18 funding scheme, with the project number K 128729.

**Data Availability Statement:** Data are contained within the article.

**Conflicts of Interest:** The authors declare no conflict of interest.

## References

1. Ring, P.; Schuck, P. *The Nuclear Many-Body Problem*; Springer: Berlin/Heidelberg, Germany, 1980.
2. Eisenberg, J.M.; Greiner, W. *Nuclear Theory I: Nuclear Models*, 3rd ed.; North-Holland: Amsterdam, The Netherlands, 1987.
3. Wong, S.S.M. *Introductory Nuclear Physics*; Wiley Verlag: Weinheim, Germany, 1998.
4. Nilsson, S.G.; Ragnarsson, I. *Shapes and Shells in Nuclear Structure*; Cambridge University Press: Cambridge, UK, 1995.
5. Williams, W.S.C. *Nuclear and Particle Physics*; Clarendon Press: Oxford, UK, 1991.
6. Draayer, J.P. *Algebraic Approaches to Nuclear Structure: Interacting Boson and Fermion Models*; Casten, R.F., Ed.; Harwood Academic Publishers: Singapore, 1993; p. 423.
7. Elliott, J.P. Collective Motion in the Nuclear Shell Model. I. Classification Schemes for States of Mixed Configurations. *Proc. R. Soc. A* **1958**, *245*, 128–145. [[CrossRef](#)]
8. Elliott, J.P. Collective Motion in the Nuclear Shell Model. II. The Introduction of Intrinsic Wave-Functions. *Proc. R. Soc. A* **1958**, *245*, 562–581. [[CrossRef](#)]
9. Elliott, J.P. *Selected Topics in Nuclear Theory*; Janouch F., Ed.; IAEA: Vienna, Austria, 1963; p. 157.
10. Harvey, M. *Advances in Nuclear Physics: The Nuclear SU<sub>3</sub> Model*; Baranger, M., Vogt, E., Eds.; Plenum Press: New York, NY, USA, 1968; Volume 1, pp. 67–180
11. Lipkin, H.J. *Lie Groups for Pedestrians*; North-Holland Publication Co.: Amsterdam, The Netherlands, 1966.
12. Rosensteel, G.; Rowe, D.J. Nuclear Sp(3, R) Model. *Phys. Rev. Lett.* **1977**, *38*, 10–14. [[CrossRef](#)]
13. Rosensteel, G.; Rowe, D.J. On the algebraic formulation of collective models III. The symplectic shell model of collective motion. *Ann. Phys.* **1980**, *126*, 343–370. [[CrossRef](#)]

14. Rowe, D.J.; Rosensteel, G. Rotational bands in the  $u(3)$ -boson model. *Phys. Rev. C* **1982**, *25*, 3236–3238. [[CrossRef](#)]
15. Castanos, O.; Draayer, J.P. Contracted symplectic model with ds-shell applications. *Nucl. Phys. A* **1989**, *491*, 349–372. [[CrossRef](#)]
16. Cseh, J. Some new chapters of the long history of  $SU(3)$ . *EPJ Web Conf.* **2018**, *194*, 05001. [[CrossRef](#)]
17. Cseh, J. Microscopic structure and mathematical background of the multiconfigurational dynamical symmetry. *Phys. Rev. C* **2021**, *103*, 064322. [[CrossRef](#)]
18. Cseh, J.; Riczu, G.; Darai, J. A symmetry in-between the shapes, shells, and clusters of nuclei. *Symmetry* **2023**, *15*, 115. [[CrossRef](#)]
19. Cseh, J. On the Logical Structure of Composite Symmetries in Atomic Nuclei. *Symmetry* **2023**, *15*, 371. [[CrossRef](#)]
20. Iachello, F. *Lie Algebras and Applications*; Springer: Berlin/Heidelberg, Germany, 2006.
21. Elliott, J.P.; Dawber, P.G. *Symmetry in Physics*; MacMillen Press: Chippenham, UK, 1986.
22. Wybourne, B.G. *Classical Groups for Physicists*; Wiley: New York, NY, USA, 1974.
23. Zhang, Z.H.; Huang, M.; Afanasjev, A.V. Rotational excitations in rare-earth nuclei: A comparative study within three cranking models with different mean fields and treatments of pairing correlations. *Phys. Rev. C* **2020**, *101*, 054303. [[CrossRef](#)]
24. Kondratyev, V.N. R-Process with Magnetized Nuclei at Dynamo-Explosive Supernovae and Neutron Star Mergers. *Universe* **2021**, *7*, 487. [[CrossRef](#)]
25. Rowe, D.J.; Wood, J.L. *Fundamentals of Nuclear Models*; World Scientific: Singapore, 2010; p. 98.
26. Brink, D.M.; Satchler, G.R. *Angular Momentum*; Oxford University Press: Oxford, UK, 1962; p. 51.
27. Goldstein, H. *Classical Mechanics*; Addison Wesley: Amsterdam, The Netherlands, 1974; p. 165.
28. Budó, Á. *Mechanika*; Tankönyvkiadó, Negyedik kiadás: Budapest, Hungary, 1965; p. 216.
29. Bohr, A.; Mottelson, B.R. *Nuclear Structure: Nuclear Deformations*; W.A. Benjamin: New York, NY, USA, 1975; Volume II.
30. Fayache, M.S.; Sharon, Y.Y.; Zamick, L. Single-particle energies and Elliott's  $SU(3)$  model. *Phys. Rev. C* **1997**, *55*, 1575–1576. [[CrossRef](#)]
31. Moya de Guerra, E.; Sarriguren, P.; Zamick, L. Analytic expressions for the single particle energies with a quadrupole-quadrupole interaction and the relation to Elliott's  $SU(3)$  model. *Phys. Rev. C* **1997**, *56*, 863–867. [[CrossRef](#)]
32. Cseh, J. Algebraic models for shell-like quarteting of nucleons. *Phys. Lett. B* **2015**, *743*, 213–217. [[CrossRef](#)]
33. Cseh, J.; Riczu, G. Quartet excitations and cluster spectra in light nuclei. *Phys. Lett. B* **2016**, *757*, 312–316. [[CrossRef](#)]
34. Riczu, G.; Cseh, J. A unified description of spectra of different configurations, deformation and energy regions. *Bulg. J. Phys.* **2021**, *48*, 524–534. [[CrossRef](#)]
35. Riczu, G.; Cseh, J. Gross features of the spectrum of the  $^{36}\text{Ar}$  nucleus. *Int. J. Mod. Phys. E* **2021**, *30*, 2150034. [[CrossRef](#)]
36. Akiyama, Y.; Draayer, J.P. A user's guide to Fortran programs for Wigner and Racah coefficients of  $SU(3)$ . *Comput. Phys. Commun.* **1973**, *5*, 405–415. [[CrossRef](#)]

**Disclaimer/Publisher's Note:** The statements, opinions and data contained in all publications are solely those of the individual author(s) and contributor(s) and not of MDPI and/or the editor(s). MDPI and/or the editor(s) disclaim responsibility for any injury to people or property resulting from any ideas, methods, instructions or products referred to in the content.